INFLUENCE OF THE FIBER ALIGNMENT IN THE BALLISTIC PERFORMANCE OF DYNEEMA NON-WOVEN FABRICS

Francisca Martinez-Hergueta[1], Francisco Gálvez[2] and Carlos González[1,2]
[1]*IMDEA Materials Institute, C/Eric Kandel, 2, 28906 Getafe, Madrid, Spain*
[2]*Department of Materials Science, Polytechnic University of Madrid, E.T.S. de Ingenieros de Caminos, 28040 Madrid, Spain*

The aim of this study was the determination of the deforming micromechanisms of needlepunched felts subjected to impact loads. A large experimental campaign has been carried out to analyze the influence of the fiber alignment in the ballistic performance. Ballistic limit curves of predeformed samples were compared. The fiber realignment was experimentally measure by means of 2D X-Ray diffraction. Higher specific absorption was observed for samples with a more isotropic mechanical response. A constitutive physically-based model was developed within the context of the finite element method, which provided the constitutive response for a mesodomain including micromechanical aspects as fiber alignment, fiber sliding and pull-out. The macroscopic response has been validated with the experimental results, showing a very good agreement. The absorbed energy by the material during the impact was predicted and the fiber realignment evolution was also obtained.

INTRODUCTION

In recent years, soft-body amour manufacturers are replacing the traditional protection systems based on ceramic/composite panels in applications such as vehicles or aircrafts armoring. Dry fabrics manufactured with high strength fibers are promising lightweight solutions and have an outstanding performance in arresting metallic fragments. The ballistic response of woven dry fabrics has been extensively reported in the literature [1]. For instance, Kevlar fabrics are currently used for barriers [2]. However, arresting small fragments with dry wovens may not be totally useful depending on the relation between the size of the fragment and the fabric architecture [3]. In those cases, non woven felts show the best ballistic performance against small fragment impacts. Fibers in non-wovens are randomly distributed in the plane. The structural behaviour is not only due to the specific stiffness and strength of the fibers but the on the way the fibers interact between each other [4]. Non-wovens felts possess slightly lower strength and stiffness than its woven counterpart, but superior energy consumption capability during deformation, in particular, when arresting small calibers.

Different nonwoven felts have been design to increase the absorbed specific energy of shields. In 1995, DSM started to commercialize Dyneema Fraglight, a felt based on ultra-high molecular weight polyethylene fibers (UHMWPE). Their mechanical quasistatic and dynamic properties had been fully characterized [5] and ballistic tests were carried out [6,7]. A very good performance to stop fragments with a very low areal density was found, although large deflections were necessary to arrest the projectile. Another example developed by Auburn University is ArmorFelt [8], which combines semi-thermoplastics aramids and thermoplastic polyethylene. The main energy dissipation mechanisms corresponded to the high strain velocity

propagation, the fibrillation of the aramid fibers, and plastic deformation and phase change induced in the polyethylene fibers.

However, the ballistic performance of nonwoven felts significantly decreases when using high calibers. Some of the most relevant parameters affecting the mechanical properties in these materials are fiber orientation distribution function and fiber entanglement. Interaction between fibers seems to play an important role. Further understanding of the micromechanisms involved during the deformation process is thus required to design new felts capable to arrest higher calibers.

The present study aims to determine the influence of microstructural parameters such as fiber distribution function, fiber entanglement and fiber orientation in the mechanical response of the felt. Quasi-static tests revealed an extremely high anisotropy level of the material. To study the influence of fiber orientation on ballistic performance, specimens oriented parallel (RD) and perpendicular (TD) to the roll direction were subjected to two pre-strain levels of 20% and 40% prior to impact. Interestingly, this led to a more isotropic mechanical behaviour in roll specimens (RD) and an evident fiber alignment in transverse specimens (TD). Ballistic tests revealed that the absorbed energy increases as the material becomes more isotropic.

Based on previous findings [9], a constitutive physically-based model was implemented in an explicit finite element code. It accounts for relevant micromechanical aspects as fiber alignment, sliding and pull-out. The macroscopic response was validated with the experimental tensile tests to determine the fiber orientation index, showing a very good agreement. The model has been also used to predict the ballistic performance of the felt, as well as the influence of the micromechanisms involved in the fracture process.

MATERIALS AND METHODS

Fabrics Characteristics

A needlepunched nonwoven felt with the commercial name Dyneema Fraglight manufactured by DSM was selected for the present research. Main properties of the felt are shown in ‘Table 1’ and fiber properties are presented in ‘Table 2’. To study the influence of fiber orientation on ballistic performance, specimens were subjected to different pre-deformed levels of 20% and 40% prior to impact to modify their fiber orientation distribution and their areal weight. A schematic drawing of the initial and final geometries is drawn in ‘Figure 1’. Interestingly, this led to a evident fiber alignment in transverse specimens. A resume of all the configurations used during the experimental campaign is shown in ‘Table 3’.

TABLE I. MATERIAL PROPERTIES OF FRAGLIGHT FELT.

Property	Value
Areal Density	190-220 g/m2
Felt Thickness	1.50 mm

TABLE II. MATERIAL PROPERTIES OF DYNEEMA SK75 FIBER.

Property	Value
Density	970 kg/m^3
Young Modulus	116GPa
Strain to Failure	3.5 %
Maximum Strength	3.6 GPa
Fiber Diameter	9 μm
Fiber Length	45-55 mm

TABLE III. DESCRIPTION OF THE SPECIMENS.

Specimen	Deformed Direction	Pre-Strain (%)	Areal Weight (g/m^2)
Baseline	--	0	200
RD-20	Roll Direction	20%	168
RD-40	Roll Direction	40%	144
TD-20	Transverse Direction	20%	168
TD-40	Transverse Direction	40%	144

2D X-Ray Diffraction

2D X-Ray diffractograms were taken using a flat plate camera attached to a Phillips 2 kW tube X-ray generator using nickel-filtered Cu K_α radiation. The technique is useful for the characterization of semicrystalline polymers. The diffraction profile is given by azimuthal integration for (110) and (200) diffractions.

Ballistic Test

A pneumatic launcher was used, with compressed air or helium up to 120 bars to impel the projectile reaching 100J of impact energy at velocities ranging from 250 to 400m/s. The projectile consists of a steel sphere with 5.56mm diameter, which implies a mass of 0.706g. A Phantom high-speed camera was used to obtain the initial and residual velocities of the projectile and measure the energy absorption capacity.

Dry fabrics were clamped along their four edges using an aluminum rigid rig. The dimensions of the free surface of the fabrics were 350x350mm2, while the fabrics dimensions were 500x500mm2. All the edges of the laminates were previously impregnated with Derakane 8084 epoxy vinyl ester resin to inhibit relative frame/fabric sliding.

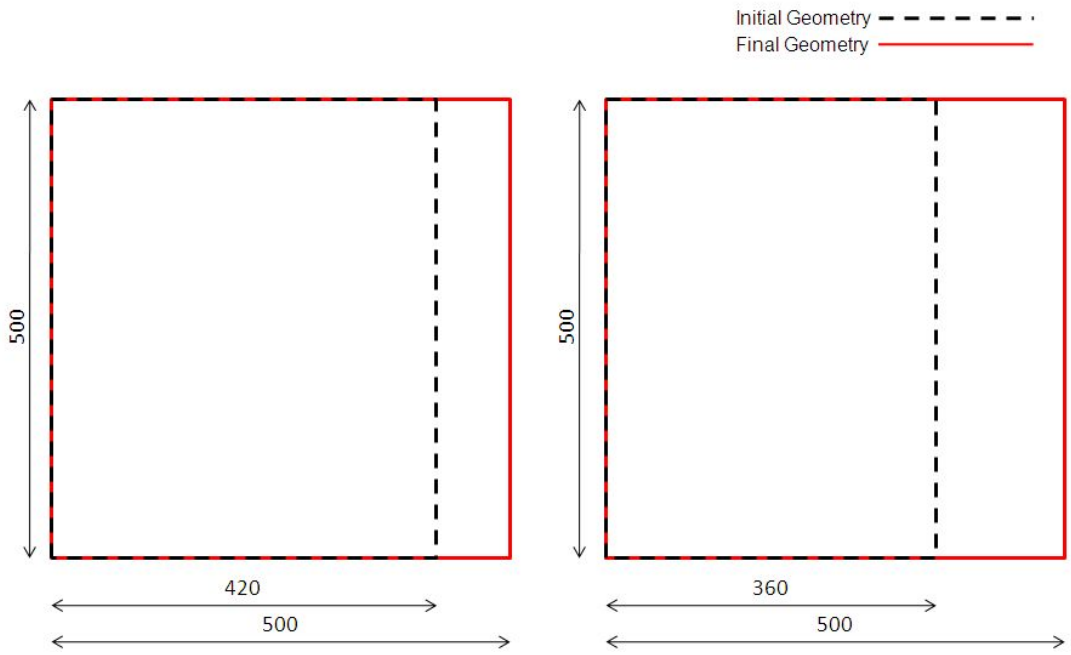

Figure 1. Initial and final geometries of the pre-tension samples, a) 20% of deformation and b) 40% of deformation.

EXPERIMENTAL RESULTS

Fiber Orientation Distribution

For the implementation of the constitutive model it was mandatory to introduce the fiber orientation distribution function (FOD). This function represented the probability of having fibers aligned in each direction [9]. As it has been observed in tensile test of the felt, the mechanical response of the material was anisotropic, being the transverse direction to the roll three times stiffer and stronger than the roll direction, 'Figure 2'.

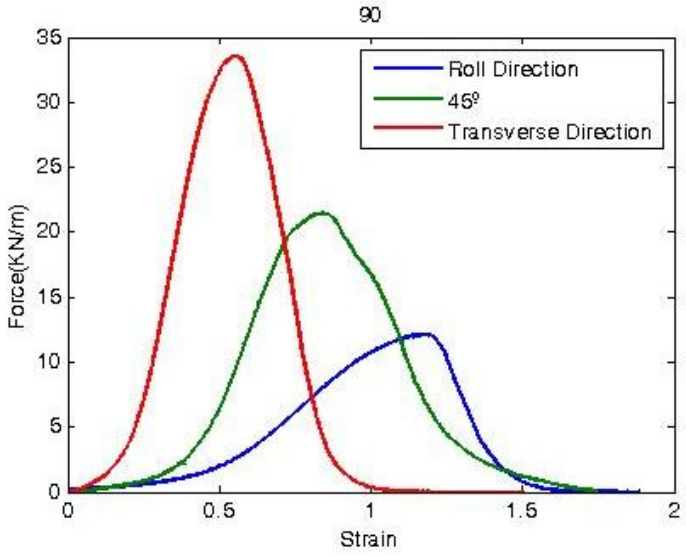

Figure 2. Load-strain curves. Felt orientation dependency.

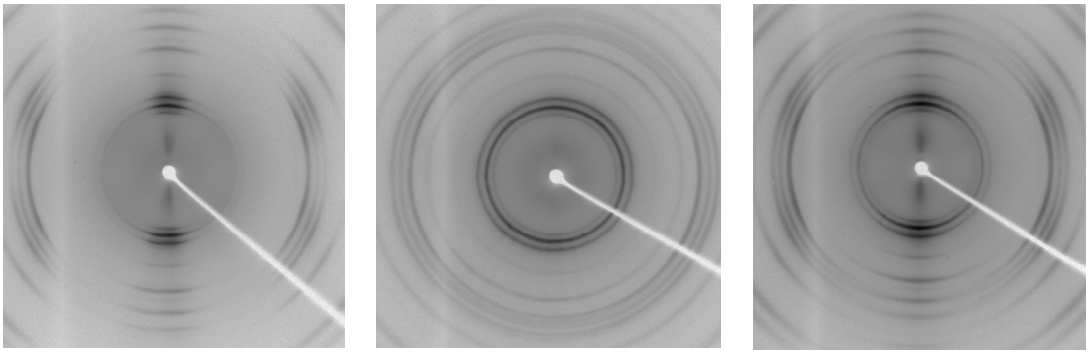

Figure 3. 2D X-Ray diffractograms, a) Dyneema fiber, b) Felt baseline and c) Predeformed sample RD40%.

The general method [10] to obtain the FOD function consisted of a microstructural analysis by means of image analysis. Photographs were usually obtained by using an optical microscope and then image analysis techniques were carried out to calculate the FOD. However this technique could only offer a view of the superficial fibers. In the present study the FOD was determined by means of 2D X-Ray diffractograms. In the following 'Figure 3' is it shown the X-Ray diffraction patterns of the single fiber, the baseline felt and a sample of the felt with 40% of deformation in the transverse direction. A characteristic pattern of spots related to the polymer crystal phase, oriented in the fiber direction, was observed for the Dyneema fiber, meanwhile for the baseline felt the dispersion along the whole azimuthal angle of these spots was found due to the different fiber orientations, resulting in an almost homogeneous ring around the center of the image.

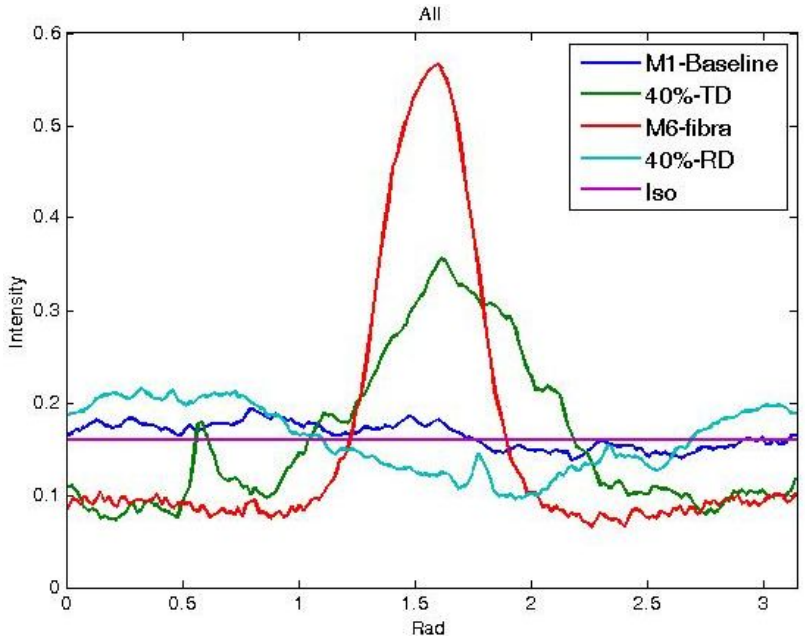

Figure 4. Fiber orientation distribution functions. Azimuthal integrations along a ring of the 2D X-Ray diffractograms for M1-Baseline felt, M6- fiber, samples with a 40% of deformation for transverse and roll direction and the theoretical isotropic fiber distribution.

As an example, results for the TD 40% layer were included and it is remarkable to observed that the pattern obtained for this sample was intermediate between the fiber and the felt baseline. All these results are plotted in 'Figure 4' and compared with the theoretical isotropy FOD finding negligible differences between the baseline felt and the theoretical. So it was concluded that for the Fraglight felt the FOD was quasi-isotropic and the anisotropy mechanical behaviour of the material had to be related to other microstructural features caused during the punching process, such as fiber entanglement or fiber curling.

Ballistic Results

Ballistic limit curves for all configurations are shown in 'Figure 5'. It was evident that all predeformed samples had a lower ballistic limit V_{50} related to the reduction of the areal weight of the samples. However samples deformed in the roll direction presented higher energy absorption above the ballistic limit. In 'Figure 6' the absorbed energy by the target vs the initial energy of the impact is shown. The red line represents the 100% of energy absorption, the orange line corresponds to the 75% and the yellow line to the 50%. It was observed that the energy absorption for the baseline felt and the samples predeformed in the TD was reduced to the 50% for velocities above the ballistic limit, meanwhile the samples predeformed in the RD were capable to absorb a higher amount of energy for a wider range of velocities.

The increment of the ductility of the material was related to the micromechanisms involved in the failure process for each sample. In 'Figure 7.a and .b' the fiber pull-out during impact for two different specimens is presented. It can be observed that samples deformed at RD presented a significant fiber pull-out, meanwhile for the samples deformed at TD the fiber pull-out was negligible. The enhancement of the ballistic performance could be even more evident if the current areal weight of the samples is included in the analysis.

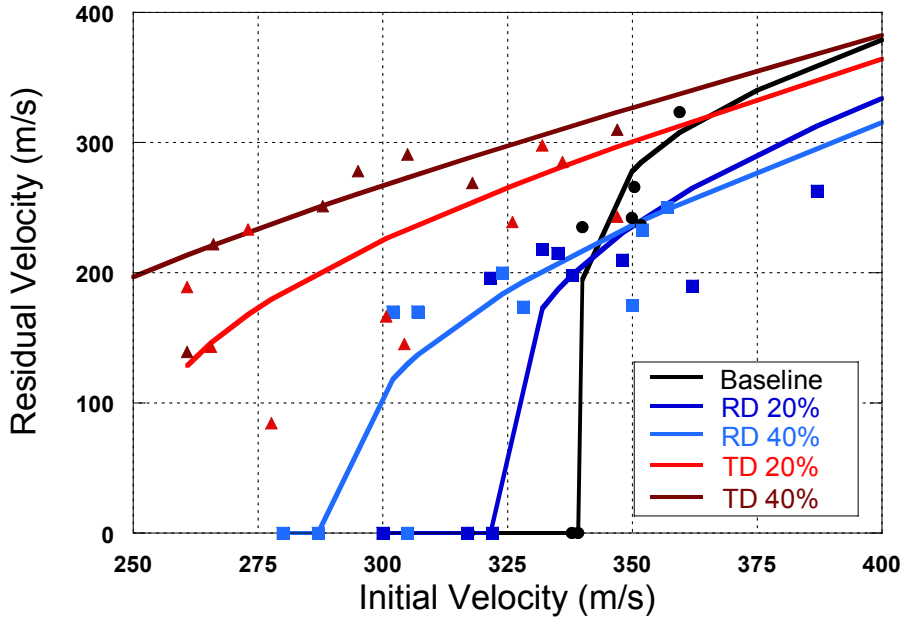

Figure 5. Ballistic limit curves for all the specimens tested.

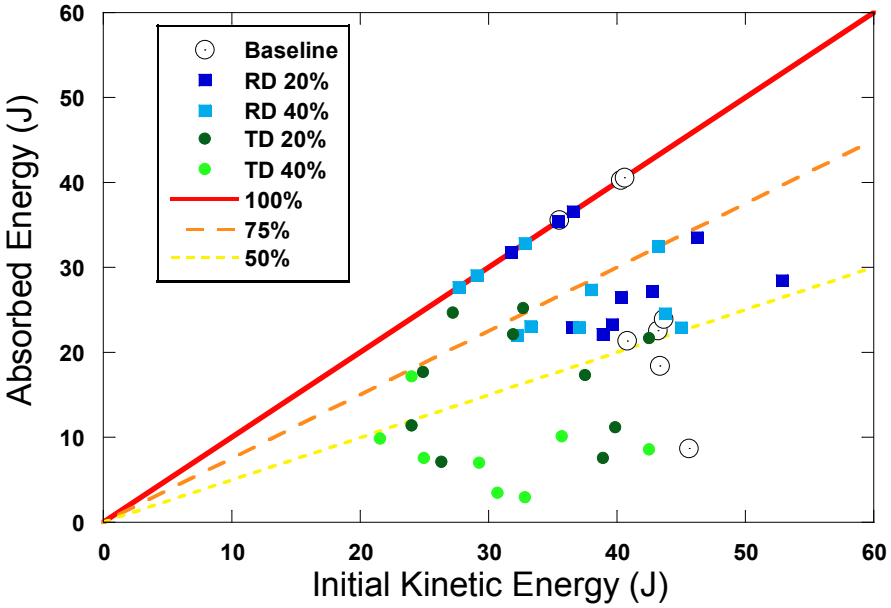

Figure 6. Ballistic performance. Absorbed energy by the target vs initial kinetic energy of the tests.

In 'Figure 7.c', the mean value of the specific energy absorption of each sample is presented. An evident enhancement of the properties while stretching in the RD was found. Even for the sample TD20% mechanical properties were still comparable to the felt baseline. It can be finally concluded that although the fiber orientation distribution of the stretched samples was not isotropic, the mechanical response against impact of the felt was more isotropic due to the combination of the new entanglement distribution and fiber alignment. All these micromechanical aspects must be taken into account to predict the failure mode of the material.

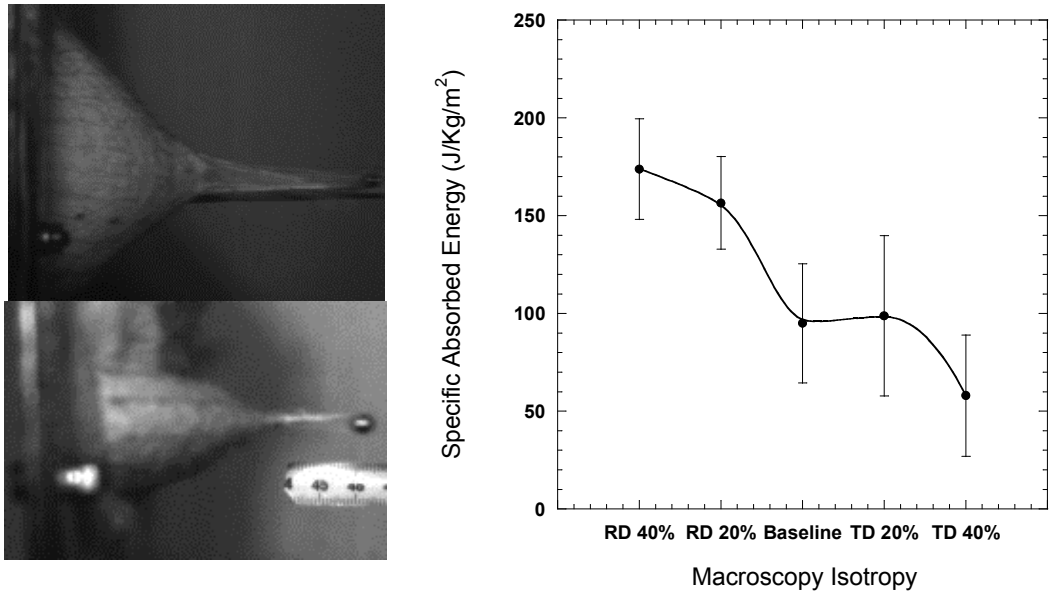

Figure 7. Ballistic Performance. In the right column a comparison between fiber pull-out for different samples, a) 20% of deformation at RD and b) 20% of deformation at TD. In the left column, c) specific absorbed energy as a function of the macroscopy mechanical response.

CONSTITUTIVE MODEL

The constitutive model used in the present work describes the mechanical response of the network in terms of non-linear elastic texture evolution related to the fiber realignment, rotation and sliding. These microstructural features are included in a tensorial representation which is embedded in a continuum formulation. The constitutive model was based on a previous study perform by Ridruejo et. al [11] and it was implemented in three different blocks; fiber network model, fiber model and damage model. For the fiber network it was needed to introduce a function with the entanglement distribution in order to obtain an anisotropic mechanical response. It was implemented by fitting the quasi-static simulations with the experimental tensile tests. The main deformation mechanisms considered for the fiber model was the fiber sliding. Pull-out tests of single fibers were carried out to characterize this micromechanism. It could be considered that one fiber crossing some fixed junctions was extracted from them while the network was clamped, 'Figure 8'. In a first stage uncurling of the fiber happened without extracting the fiber from the entanglements. Once the fiber was totally uncurled, in the second stage, adjacent fibers were pulled with the rest, increasing the stresses in the bonds. In the last stage, as the bond strength was overtaken, sliding of the fiber took place and fiber disentanglement produced the felt failure.

To obtain such mechanical behaviour the stress-stretch function for a single fiber was computed as function of the pull-out length and of the fiber orientation respect a privileged direction θ, see equation 2. With this formulation the resistance to fiber sliding was increased for higher deformations. Disoriented fibers perpendicular to the loading direction will be easily extracted from the felt by the slippage pull-out mechanical behaviour.

$$s_f = s_f^{po} \tag{1}$$

$$s_f^{po} = E_{po}\left(e_{po},\theta\right)\cdot e_{po}\,; \qquad E_{po} = K\cdot e_{po}^2\cdot\left(1-\sin^4\theta\right) \tag{2}$$

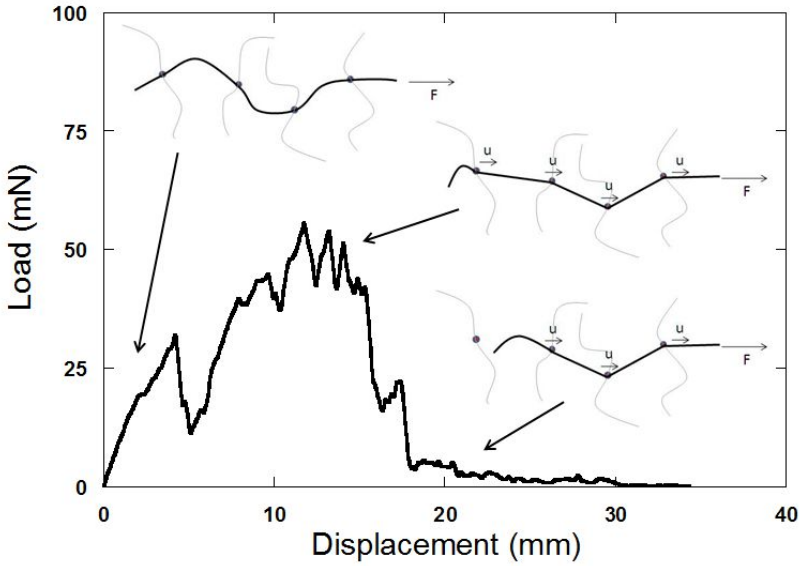

Figure 8. Deforming micromechanisms represented on a typical load-displacement pull-out curve. Stage 1, fiber uncurling. Stage 2, pulling of adjacent fibers. Stage 3, disentanglement.

The instant fiber alignment was registered by the orientation index β;

$$\beta = \int_{-\frac{\pi}{2}}^{\frac{\pi}{2}} \frac{FN^{\theta}}{\left\| FN^{\theta} \right\|} \cdot e_1 \Psi(\theta) d\theta \tag{3}$$

where e_1 is the unit vector along a privileged direction. According to this definition, total perpendicular alignment of fibers to the reference direction will result in β=0 while total fiber alignment to the reference direction will result in β=1.

For the damage model, maximum strength to pull-out of the fibers was a random value inside an interval given by the experimental pull-out test. The maximum pull-out strength for each set of fibers in the mesodomains was implemented with a Monte Carlo lottery method. With this method it was represented the random nature of fiber connectivity and junctions.

The model was implemented as a VUMAT subroutine in Abaqus/Explicit and all predictions correlated quite well with the experimental results. In 'Figure 9' correlation between the absorbed energy by the baseline felt is presented. Ballistic limit V_{50} and energy absorption for velocities above the V_{50} are well predicted. In 'Figure 10' a comparison between the pull-out damage shows a very good correlation. Finally, in 'Figure 11' the analysis of the fiber orientation is shown. The predicted fiber alignment for the samples deformed at TD was nearly total at the line which connected the edges of the clamp. A similar result was observed by means of 2D X-Ray diffraction.

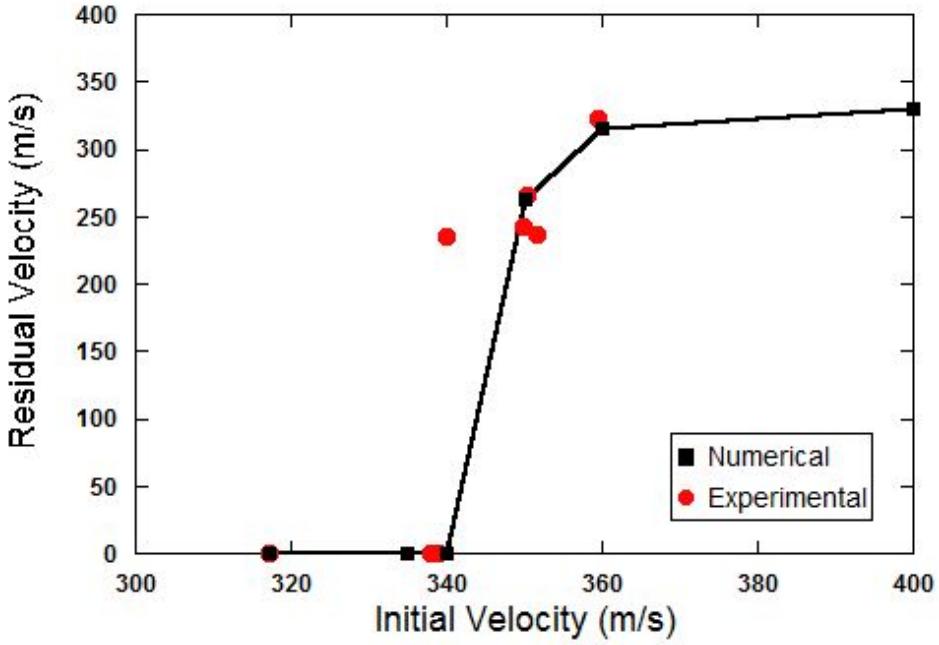

Figure 9. Correlation between experimental and numerical results for ballistic limit curves.

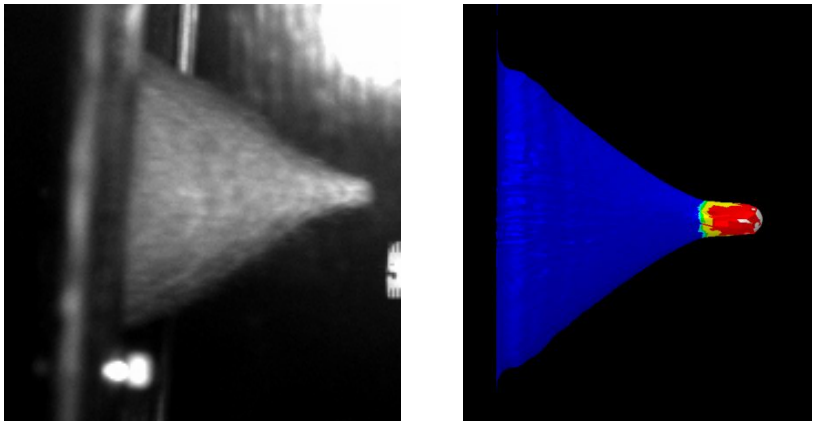

Figure 10. Correlation between experimental and numerical results. Pull-out damage caused during an impact at V=300m/s.

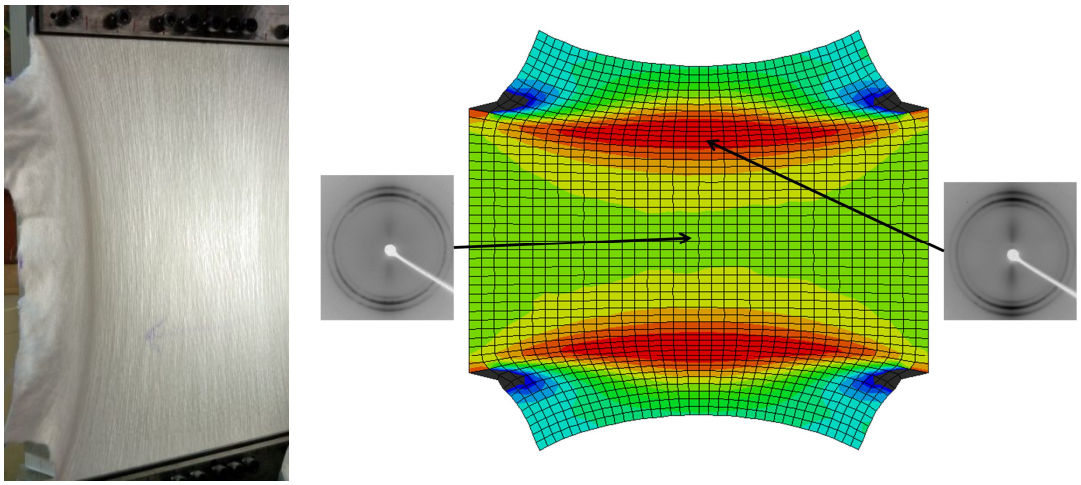

Figure 11. Correlation for fiber alignment. a) Photo of a sample deformed at TD, b) Numerical prediction and 2D X-Ray diffractograms. Prediction of the fiber alignment and fiber density.

CONCLUSIONS

This paper has given an account of the ballistic performance of needle punched nonwoven felt. A large experimental campaign has been carried out to fully characterize the mechanical response. A novel experimental technique was applied for the measurement of the fiber alignment based on 2D X-Ray diffraction. The influence of the fiber alignment in the ballistic performance was study in samples with a predeformation prior to impact. Deforming micromechanisms during impact were experimentally observed and detailed analyzed. Higher pull-out was found for samples stretched into the RD. It was concluded that the ballistic performance of nonwoven felts could be enhanced by changing the fiber orientation distribution into a more isotropic bond distribution. The relevance of fiber sliding and pull-out in the energy absorption capacity of the material is clearly supported by the current findings.

A physically-based continuum model was developed. It provides the behaviour of the felt at the mesodomain level and has been implemented as a material subroutine within the framework of the finite element methods. The mechanical response of each bundle was described in terms of fiber sliding and disentanglement. These findings suggested that in general the mechanical response of the felt depended on the fiber

network rather than in fiber properties. Numerical predictions of the tensile test and impact tests were obtained with and Abaqus/Explicit implementation of the constitutive model. Most of the fiber parameters were obtained from the previous experimental characterization. Good correlation of the ballistic limit V_{50} and absorbed energy was obtained and the pull-out damage pattern was reproduced as well. Prediction of the fiber distribution evolutions were in good correlation with the experimental measurements. The results showed the potential of this physically-base model to reproduce the complex deformation and fracture micromechanisms of nonwoven needle punched fabrics.

ACKNOWLEDGEMENTS

This investigation was supported by the Spanish Ministry of Education through grant FPU12/02087. The financial support that the Spanish Center for Industrial and Technological Development CDTI has given through the Projects TARGET (CENIT program) and BIA2011-24445 is greatly acknowledged. The brilliant collaboration of A. Ridruejo and J.P. Fernandez-Blazquez is also gratefully acknowledged.

REFERENCES

[1] P. M. Cunniff "An analysis of the system effects in woven fabrics". *Textile Research Journal*, Vol 62, No. 9, pp 495–509, 1992.

[2] D. Naik, S. Sankaran, B. Mobasher, S. Rajan and J. Pereira "Development of reliable modeling methodologies for fan blade out containment analysis – Part I: Experimental studies". *International Journal of Impact Engineering*, Vol 36, No. 1, pp 1–11, 2009.

[3] B. Cheeseman "Ballistic impact into fabric and compliant composite laminates". *Composite Structures*, Vol 61, pp 161–173, 2003.

[4] A. Ridruejo, C. González and J. LLorca "Failure locus of polypropylene nonwoven fabrics under in-plane biaxial deformation" *Comptes Rendus Mécanique,* Vol 340, Issues 4-5, pp 307-319, 2012.

[5] S. Chocron, A. Pintor, F. Gálvez, C. Roselló, D. Cendón and V. Sánchez-Gálvez "Lightweight polyethylene non-woven felts for ballistic impact applications: Materials characterization" *Composites Part B: Engineering,* Vol 39, No 1, pp 1240-1246, 2008.

[6] S. Chocron and A. Pintor "Simulation of ballistic impact in a polyethylene non-woven felt". *20Th Internationa Symposium on Ballistics*, Orlando, FL pp. 23–27, 2002.

[7] Russell, S. J., Pourmohammadi, a., Ezra, I., & Jacobs, M. (2005). Formation and properties of fluid jet entangled HMPE impact resistant fabrics. *Composites Science and Technology*, *65*(6), 899–907.

[8] G.A. Thomas. "Non-woven fabrics for military applications" *Military Textile,* Edited by Eugene Wilusz, pp 44-47. Cambridge, England: Woodhead Publishing, Ltd.

[9] A. Raina and C. Linder. A homogenization approach for nonwoven materials based on fiber undulations and reorientation. *Journal of the Mechanics and Physics of Solids*, *65*, 12–34, 2014.

[10] Farukh, F., Demirci, E., Sabuncuoglu, B., Acar, M., Pourdeyhimi, B., & Silberschmidt, V. V. Numerical analysis of progressive damage in nonwoven fibrous networks under tension. *International Journal of Solids and Structures*. Accepted Manuscript. 2014.

[11] A. Ridruejo, C. Gonzalez, and J. LLorca. A constitutive model for the in-plane mechanical behavior of nonwoven fabrics. *International Journal of Solids and Structures*, 49(17):2215-2229, September 2012.